Applied Radiation and Isotopes 176 (2021) 109893

Contents lists available at ScienceDirect

Applied Radiation and Isotopes

journal homepage: www.elsevier.com/locate/apradiso

Ytterbium-175 half-life determination

M. Teresa Durán [a,*], Frédéric Juget [a], Youcef Nedjadi [a], François Bochud [a], Zeynep Talip [b], Nicholas P. van der Meulen [b,c], Ulli Köster [d], Charlotte Duchemin [e,f], Thierry Stora [e], Claude Bailat [a]

[a] Institute of Radiation Physics, Lausanne, Switzerland
[b] Center for Radiopharmaceutical Sciences ETH-PSI-USZ, Paul Scherrer Institute, Villigen-PSI, Switzerland
[c] Laboratory of Radiochemistry, Paul Scherrer Institute (PSI), Villigen-PSI, Switzerland
[d] Institut Laue-Langevin (ILL), Grenoble, France
[e] European Organization for Nuclear Research (CERN), Geneva, Switzerland
[f] KU Leuven, Instituut voor Kern-en stralingsfysica (IKS), B-3001 Leuven, Belgium

ARTICLE INFO

Keywords:
^{175}Yb
Half-life
Standardization
Ionization chamber
Digital electronics.

ABSTRACT

^{175}Yb is a radionuclide that can be generated by neutron capture on ^{174}Yb and whose decay properties make it useful for developing therapeutic radiopharmaceuticals. As it happens with many of the emerging radionuclides for medical uses in recent years, its nuclear data were determined decades ago and are not thoroughly documented nor accurate enough for metrological purposes. The last documented reference for the ^{175}Yb half-life value is 4.185(1) days and dates back to 1989, so a redetermination of the value was considered appropriate before standardization at the Institute of Radiation Physics (IRA, Lausanne, Switzerland) primary measurements laboratory. Three independent measurement methods were used to this purpose: reference ionization chamber (CIR, *chambre d'ionization de référence*), $CeBr_3$ γ-ray detector with digital electronics and a second $CeBr_3$ detector with analog electronics and single-channel analyzer (SCA) counting. The value obtained for the ^{175}Yb half-life is 4.1615(30) days which shows a 0.56% relative deviation to the last nuclear reference value (ENSDF 2004) and is supported with a detailed calculation of the associated uncertainty.

1. Introduction

^{175} Yb decays by β^- particle emission (Q_{β^-} = 470.1(12) keV (Meng Wang 2021) to stable ^{175}Lu emitting mainly 113.8 keV (3.87(5)%), 282.5 keV (6.13(8)%) and 369.3 keV (13.2(3)%) gamma rays (ENSDF), suitable for studying bio-localisation (Chakraborty 2002). It presents excellent decay properties for developing various radiotherapeutic agents (Jamre et al., 2019; Vaez-Tehrani et al., 2016; Aghaei-Amirkhizi et al., 2016; Aghanejad et al., 2014; Vahidfar et al., 2014; Mathew et al., 2004). A traceability chain to the SI unit of radioactivity along with the fundamental nuclear data is essential to allow the development and application of radionuclides in nuclear medicine. In particular, the last documented reference of ^{175}Yb half-life dates back from 1989 (Abzouzi et al., 1989), which is the reference for the stated value in the last Nuclear Data Sheets (NDS) for A = 175 from 2004 (Shamsuzzoha Basunia, 2004). The measured value is 4.185(1) days. There is only one more measurement of ^{175}Yb half-life from a publication dated in 1966 (Wien, 1966) stating a value of 4.19(1) days. Due to the shortage of precise measurements and in order to obtain a more detailed uncertainty assessment, we decided to remeasure the half-life value of ^{175}Yb, with the aim of contributing to the metrological quality of the traceability chain.

2. Experimental conditions

2.1. Source preparation

Enriched $^{174}Yb_2O_3$ (98.16%, ISOFLEX, USA) was used as target material for the production of ^{175}Yb via the ^{174}Yb (n,γ) ^{175}Yb nuclear reaction. Irradiation was performed at the high-flux research reactor of Institute Laue–Langevin (ILL), Grenoble, France (thermal neutron flux at the irradiation position ≈ $1.1{\cdot}10^{15}$ n·cm^{-2}·s^{-1}). After irradiation, the sample was transported to the CERN-MEDICIS facility (Duchemin, 2020) for the offline mass separation of mass 175. Then, it was

* Corresponding author.
E-mail address: teresa.duran@chuv.ch (M.T. Durán).

https://doi.org/10.1016/j.apradiso.2021.109893
Received 7 June 2021; Accepted 8 August 2021
Available online 10 August 2021

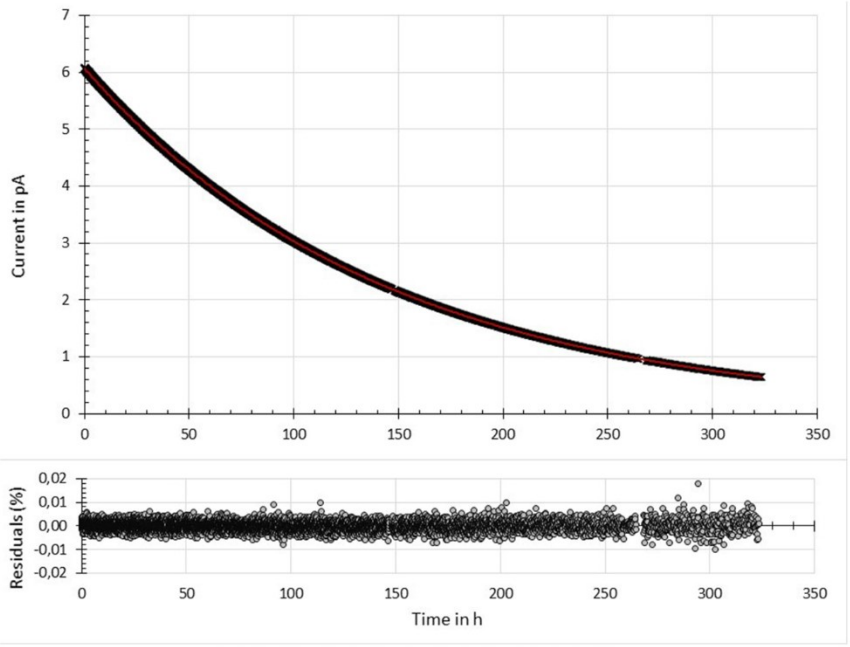

Fig. 1. ^{175} Yb day curve (×) measured with the CIR and exponential fit (−). In the graph below the residuals from the fit in % are presented. The horizontal axis is common to both graphs.

chemically purified at the Paul Scherrer Institute (PSI) and diluted with a stable carrier (Talip et al., 2021). A sample consisting of 1 g of 25 μg/g $YbCl_3$ in 0.1 M HCl solution was received at IRA with an activity of about 4 MBq. It was diluted by a factor of 3.9 using the same carrier to prepare one source in a glass ampoule, three solid sources, five liquid scintillation sources, and two liquid sources for γ-ray spectrometry.

A glass ampoule was filled gravimetrically with 3 g of the solution. Its activity was approximately 3 MBq at the reference date. This ampoule was measured with the reference ionization chamber (CIR) at IRA, which was previously used for half-life measurements of ^{137}Cs and ^{161}Tb (Juget et al., 2016; Duran et al., 2020).

Two solid sources were gravimetrically prepared for gamma-counting with $CeBr_3$ detectors. Two aliquots of 83.11(2) and 84.56(2) mg of the $YbCl_3$ were deposited with a pycnometer onto two plastic supports and then left to dry.

Other solid and liquid scintillation sources were prepared for exploratory plastic and liquid scintillation standardization tests, respectively. Two vials filled with the carrier solution and aliquots of the radioactive solution were also prepared to check for impurities by HPGe γ-ray spectrometry.

2.2. $CeBr_3$ detector with digital electronics

The γ-ray $CeBr_3$ detector is a Scionix 51B51/2M-CEBR-E1. It is a cylindrical $CeBr_3$ crystal, 2 inch in diameter and 2 inch in length, integrally coupled to a photomultiplier tube operated at 650 V. This detection system is housed at the bottom of a 50-cm-diameter and 5-cm-thick cylindrical shield covered with a sliding square (6-cm-thick armoured plate). The anode signal is connected to a dedicated Scionix preamplifier Amp-1000-E2 from where the output signal is collected, digitized and treated with a National Instruments (NI) digital electronics system, as described elsewhere (Duran et al., 2020).

2.3. $CeBr_3$ detector with analogue counters

Another γ-ray $CeBr_3$ detector and preamplifier assembly, identical to the one described in the previous section, using analogue electronics for counting the number of events above a gamma energy threshold, was used for the half-life measurement. The plastic support carrying the dry radioactive deposit was placed directly on the centre-top of the detector, which was housed at the bottom of a 32-cm-diameter and 5-cm-thick cylindrical shield.

The signal from the preamplifier was treated by an amplifier Canberra 2024 and fed into a Canberra 2037A single-channel analyzer with pulse lockout logic that minimises out-of-channel event dead-time. The pulses from this module were duplicated so that one train of pulses would be fed into a 50 μs non-extending dead-time generator, while the other would undergo about 150 μs dead-time imposition. The dead-time enforcement was obtained by combining an Ortec CO4020 input logic with a Philips 794 gate and delay generation. The resultant non-extending dead-times were measured precisely using the two-oscillator method (Gostely, 1978). The two signals were sent to the integrated 32-bits counter/timer PCI-6602 device from National Instruments, to count the number of γ-rays above an energy threshold set in the single-channel analyzer. An automated acquisition program using LabVIEW software recorded the number of counts in each channel, as well as the starting time and counting time of each measurement. The counting time is calculated by counting the frequency pulses from the DCF77 frequency standard type 860 (DCF77, 2021), which gives a high-stability frequency at 10 MHz, 1 MHz and 100 kHz with an accuracy of 10^{-8} for 10 s measuring time.

2.4. Radionuclidic impurity

The solution was measured by γ-ray spectrometry with a high-purity Ge (HPGe) detector to search for any potential impurities. The source was measured over a period of five days and no radionuclidic impurities were detected.

3. Measurement procedures and results

3.1. Ionization chamber current measurements

The source was placed inside the chamber to be measured over a period of two weeks, approximately five times the ^{175}Yb half-life. 6970 measurements were performed consecutively over this period. The time

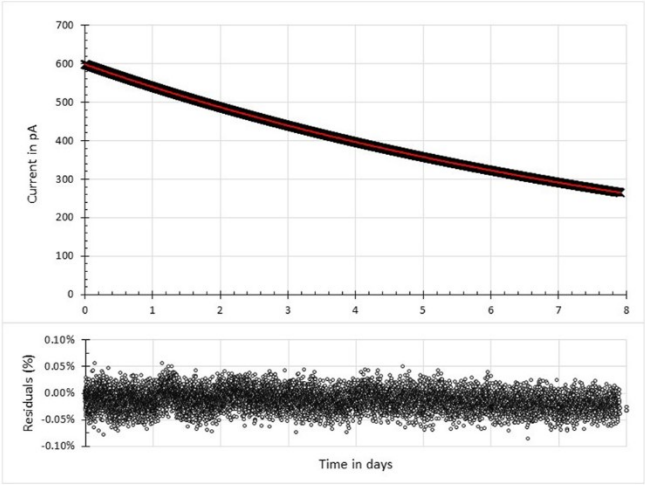

Fig. 2. ^{177}Lu decay curve (×) measured with the CIR and double exponential fit (–). In the graph below the residuals from the fit in % are presented. The horizontal axis is common to both graphs.

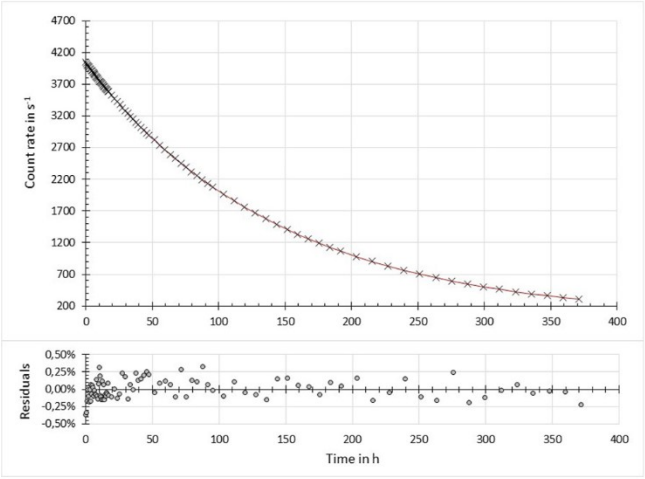

Fig. 3. ^{175} Yb day curve measured with the $CeBr_3$ detector with digital electronics. Measured data corresponding to net count rate (×) and exponential curve fit (–) are presented together with the residuals of the fit below.

needed to perform each measurement changed over the period beginning at 51 s and ending at almost 9 min. The current measurement principle is described in (Juget et al., 2016; Duran et al., 2020). The current was measured and corrected for saturation, background and decay during the measurement using the reference value from the last NDS (4.185 d).

A simple exponential decay curve [1] was fitted to the measurement current (I_c) as no contribution from impurities was detected.

$$I_C(t) = I_C(0)\cdot e^{-\lambda_{175}\cdot t} \quad [1]$$

The decay curve, exponential fit and its residuals are shown in Fig. 1. The result obtained for the ^{175}Yb half-life was 4.1602(21) days.

3.2. Validation of the ionization chamber measurements using ^{177}Lu and ^{99m}Tc

In order to validate and back-up the measurements performed with the CIR, the well-known half-lives of ^{177}Lu (6.6443(9) days (Kondev, 2019) and ^{99m}Tc, (6.0072(9) hours (Browne and Tuli, 2017)) were also measured, respectively, giving compatible values: 6.640(9) days for ^{177}Lu and 6.0050(33) hours for ^{99m}Tc.

3.2.1. ^{177}Lu half-life measurement

The carrier-added (c.a.) ^{177}Lu sample was taken from a Lutathera commercial source provided by the Advanced Accelerator Applications Company (AAA). The mother sample was a solution of 22.2 mL with around 8 GBq from which an aliquot was diluted to a concentration of 78.34(27) MBq/g. An ampoule was filled with 2.925(1) g of this solution to provide an activity of 229.1(9) MBq at the beginning of the measurement. The solution was measured by γ-ray spectrometry and an impurity of ^{177m}Lu was found with an activity ratio of $2.72(9)\cdot10^{-4}$ ^{177m}Lu/^{177}Lu at the beginning of the measurement. The estimated current produced by the ^{177m}Lu impurity was less than 10^{-2} times the current produced by the ^{177}Lu at the start of the measurement.

The total activity of the sample decays as the sum of two exponentials of unknown amplitudes (Pommé et al., 2011). Therefore a double exponential function was fitted to the measured current:

$$I(t) = A\cdot e^{-\lambda_{Lu-177}\cdot t} + B\cdot e^{-\lambda_{Lu-177m}\cdot t} \quad [2]$$

where A, B and λ_{Lu-177} are free parameters and $\lambda_{Lu-177m}$ is fixed at its corresponding value from the nuclear database, 160.4(3) days (Kondev, 2019).

The measurement data and corresponding fit and residuals are presented in Fig. 2. The measured ^{177}Lu half-life is 6.640(9) days, which is in good agreement with the NDS value of 6.6443(9) days. The corresponding uncertainty was estimated in a similar way as described in section 4.1 by following the approach adopted by Pommé (Pommé et al., 2008). The residuals of the fit, the background, timing and uncertainty on the current measurement were the more significant components taken into account.

3.2.2. ^{99m}Tc half-life measurement

The ^{99m}Tc sample was obtained from the radionuclide generator PERTECTOR 2.3–57.1 GBq, provided by the Radioisotope Centre POLATOM in Poland, had a ^{99}Mo activity of 36.5 GBq at the reference time. A 5 mL sample was taken 3 days later with an activity of around 1.3 GBq. An aliquot of 4.5 g was transferred into an ampoule for the CIR measurement, which started one day after. The solution was measured by γ-ray spectrometry system at IRA and an impurity of ^{99}Mo was found with an activity ratio of $7.68(28)\cdot10^{-5}$ at the beginning of the measurement. The current produced by the ^{99}Mo impurity was estimated to be less than 10^{-5} times the current produced by the ^{99m}Tc at the start of the measurement.

Here, again, the fit function is a double exponential with unknown amplitudes:

$$I(t) = A\cdot e^{-\lambda_{Tc-99m}\cdot t} + B\cdot e^{-\lambda_{Mo-99}\cdot t} \quad [3]$$

where A, B and λ_{Tc-99m} are free parameters and λ_{Mo-99} is fixed at 65.924 (6) h (Browne and Tuli, 2017).

The fitted ^{99m}Tc half-life was 6.0050(33) hours, which is in good agreement with the NDS value, 6.0072(9) hours (Browne and Tuli, 2017). The uncertainty was, again, estimated following the Pommé approach (Pommé et al., 2008) with the following components: residuals of the fit, the background, timing and uncertainty on the current measurement.

3.3. $CeBr_3$ γ-ray spectroscopy

Two similar $CeBr_3$ detectors from the same Scionix family (51B51/2M-CEBR-E1) were used with different electronic configurations as described in sections 2.3 and 2.4.

For the detector with digital electronics, the solid source was placed on the centre top of the detector window in a fixed position, so that the measurement geometry would remain invariable during the campaign. The source was measured at regular intervals over a two-week period. The measurement time was adapted to the decreasing activity of the

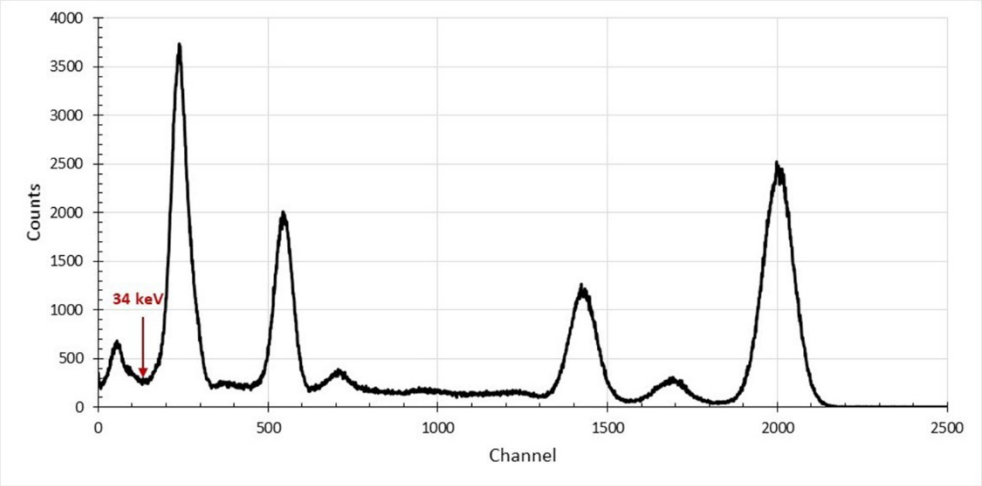

Fig. 4. ^{175}Yb energy spectrum measured with the $CeBr_3$ detector with digital electronics. The 34 keV low-level threshold for the counting area is indicated.

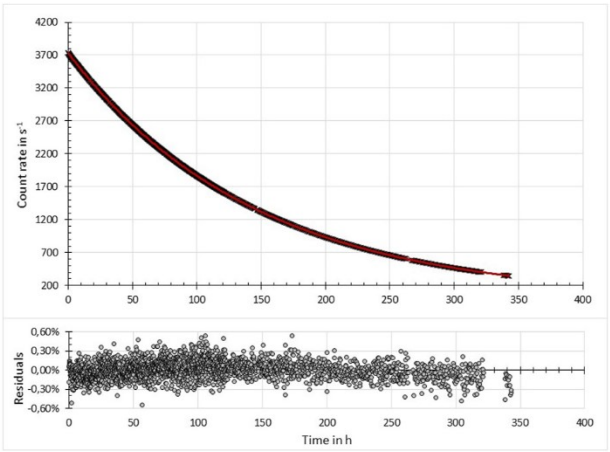

Fig. 5. Decay curve measured by the $CeBr_3$ system with 150 μs dead-time counting.

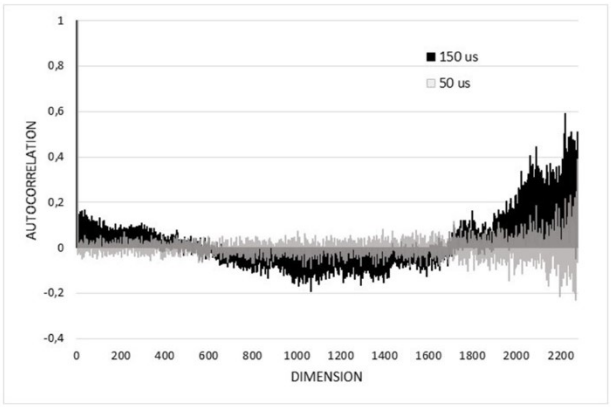

Fig. 6. Autocorrelation plots of the residuals corresponding to the decay curve fits for the 50 (grey) and 150 (black) μs dead-time counting systems.

source in order to obtain around 1 million counts per measurement to ensure the counting statistics uncertainty component remained limited to 0.1%.

After completing the measurements, the data were analysed offline. The net count rates used to form the decay curve (Fig. 3) corresponded to the area of the spectrum above 34 keV on (Fig. 4), including the main γ-ray emissions, corrected by the background measurement.

The exponential curve expressed in equation [4] was fitted to net count rate data and the value obtained for ^{175}Yb half-life was 4.1650(43) days.

$$\rho(t) = \rho(0) \cdot e^{-\lambda_{175} \cdot t} \cdot \frac{1 - e^{-\lambda_{175} \cdot \Delta t}}{\lambda_{175} \cdot \Delta t} \quad [4]$$

The fraction in the formula is the factor accounting for the decay during the measurement, where Δt is the measurement duration.

The $CeBr_3$ detector with analogue electronics and counters performed 2304 consecutive measurements ranging from 5 min at the beginning to 20 min measurement time at the end of the campaign that lasted 14 days. The counting was performed with a gamma-energy threshold of 34.7 keV and two different imposed dead-times, 50 and 150 μs, to allow for dead-time counting correction. To prevent from deviations on the gain stability, a dynamic correction of the threshold was performed for every measurement.

Fig. 5 shows the results obtained with 150 μs dead-time counting, together with the exponential fit and residuals.

The exponential curve used for fitting to the data was the same as the one in [4].

When looking at the residuals in Fig. 5, a deviation was observed. This is confirmed by the autocorrelation plots (Fig. 6), where an oscillation was clearly identified in the plot corresponding to this latter decay curve fit (150 μs dead-time).

This oscillation points out the influence of a medium frequency perturbation. One of the factors that could perturb the residuals with that kind of oscillation is the dead-time correction, so we varied numerically the dead-time value to perform the count rate correction and obtain a fitted curve that corrected the residuals. The value obtained for the dead-time was 152.5 μs, which showed clearly that the dead-time value of 150 μs was not correct.

A calibration of the dead-time module was then performed with the two-oscillator method (Gostely, 1978). The measured values were 151.576(85) μs and 50.029(9) μs and were applied to the count rate and data fit. The half-life values obtained were 4.1634(51) days and 4.1647 (8) days, respectively. Fig. 7 shows the three sets of residuals corresponding to the fits when using the module nominal, estimated and measured dead-time values for the measurement with 150 μs. Fig. 8 shows the results obtained with 50 μs dead-time counting, together with the exponential fit and residuals.

The use of the estimated and measured dead-time resulted in very similar appearances of the residuals and autocorrelation. Nevertheless, an oscillation of higher frequency remained in the autocorrelation plots,

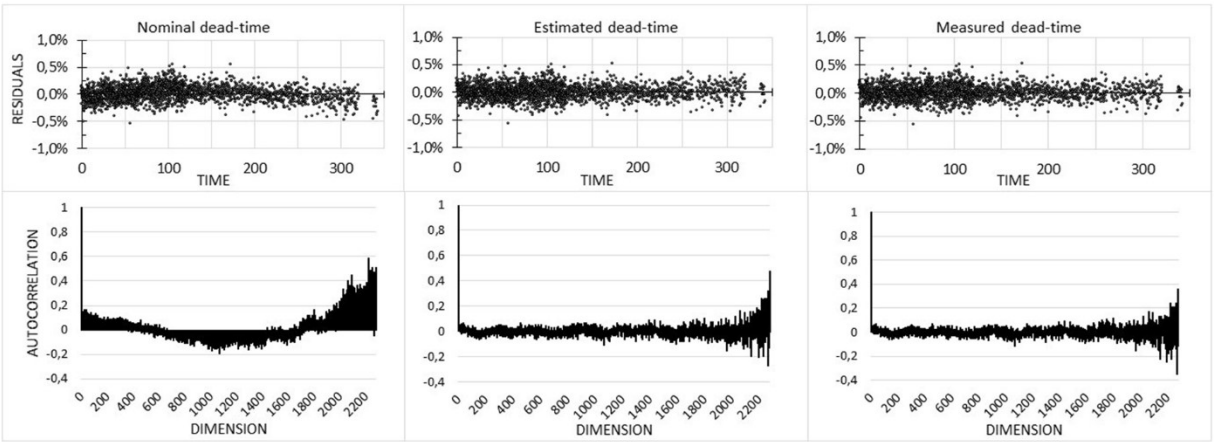

Fig. 7. Fit residuals and their corresponding autocorrelation plots below. From left to right, the graphs correspond to the sets of data calculated using the different dead-times studied: the electronic module nominal value, the estimated value and the measured value using the two-oscillator method.

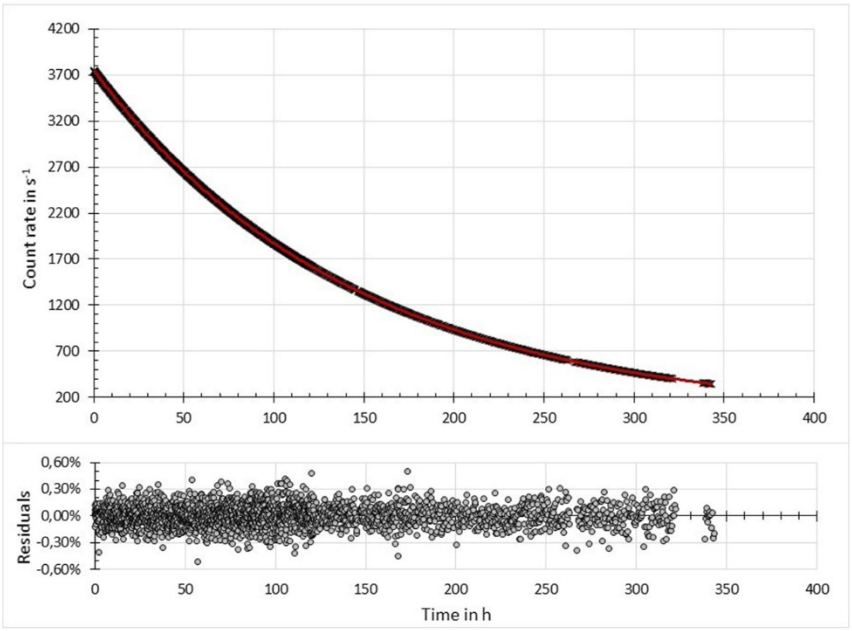

Fig. 8. Decay curve measured by the $CeBr_3$ system with 50 μs dead-time counting.

Table 1
Uncertainty budgets for each measurement and corresponding half-life values.

Uncertainty components	CIR			$CeBr_3$ digital			$CeBr_3$ analogue		
	Factor	σ(I)/I	$\sigma(T_{1/2})/T_{1/2}$	Factor	σ(N)/N	$\sigma(T_{1/2})/T_{1/2}$	Factor	σ(N)/N	$\sigma(T_{1/2})/T_{1/2}$
High-frequency									
Counting statistics	–	–	–	0.136	0.107%	0.015%	0.030	0.152%	0.005%
Residuals std. dev.	0.018	0.211%	0.004%	–	–	–	–	–	–
Medium-frequency									
Trends in residuals*	–	–	–	–	–	–	0.454	0.25%	0.114%*
Low-frequency									
Background	0.891	0.040%	0.036%	0.752	0.136%	0.102%	0.840	0.004%	0.0003%
Timing	0.891	0.040%	0.036%	0.752	0.0004%	0.0003%	0.840	0.011%	0.009%
Dead time	–	–	–	0.752	0.006%	0.004%	0.840	0.031%	0.026%
Mean									0.022%
Combined uncertainty			**0.050%**			**0.103%**			**0.120%**
$T_{1/2}$ value in days	**4.1602(21)**			**4.1650(43)**			**4.1641(50)**		

The (*) indicates values corresponding only to the measurement performed with 150 μs nominal dead-time.

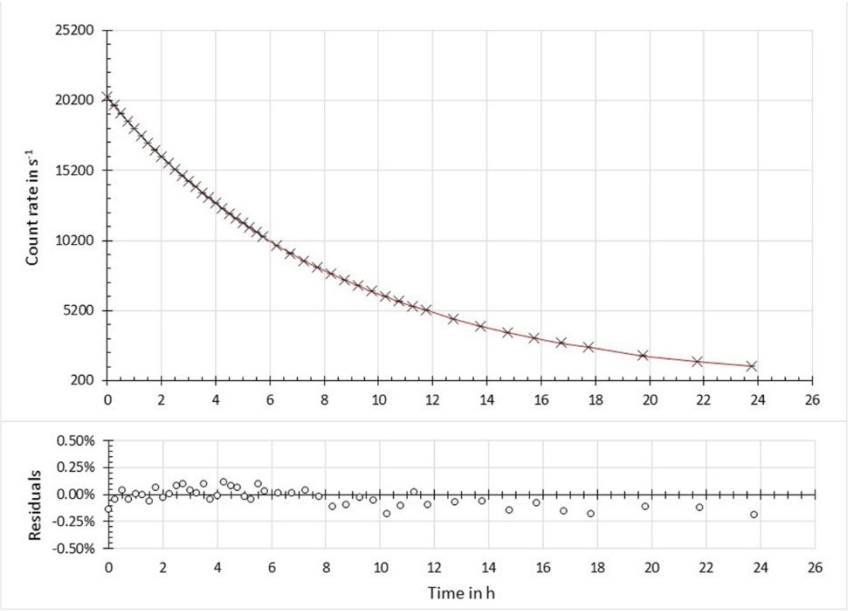

Fig. 9. ^{99m}Tc decay curve measured with the $CeBr_3$ detector with digital electronics. Measured data corresponding to net count rate (×) and exponential curve fit (−) are presented together with the residuals of the fit below.

indicating another perturbation. In this case, the origin of this perturbation could not be found. As a result, it was accounted for in the uncertainty budget (Table 1) with an additional medium-frequency component.

In Table 1, the mean value for the half-life obtained with this γ-ray spectrometry method using analogue electronics was determined to be 4.1641(50) days.

3.4. Validation of the $CeBr_3$ detector with digital electronics measurement technique using ^{99m}Tc

The well-known half-life of ^{99m}Tc, 6.0072(9) hours (Browne and Tuli, 2017), was also measured with the $CeBr_3$ digital γ-ray spectrometry system to check the appropriateness of the technique.

A ^{99m}Tc solid sample was prepared in the same way as described in section 2.1 and measured 46 times over a period of about 4 times the half-life (24 h). The result obtained from the exponential fit (Fig. 9), after no significant impurities were detected with the HPGe system, was 6.0066(61) hours, which is in good agreement with the reference value.

4. Determination procedure and discussion

4.1. Uncertainty evaluation

The uncertainty evaluation was performed following the approach by (Pommé et al., 2008) where uncertainty components were classified into high, medium and low-frequency depending on the rate at which they occur compared to the duration of the measurement campaign. Table 1 presents the uncertainty budget, where each component is calculated as the relative uncertainty affecting the measured magnitude (counts N, or current I) multiplied by a propagation factor that takes into account the real impact of these perturbations along the measurement period and the fitting procedure.

To account for the propagation factors into the half-life value, the formula from (Pommé, 2015) was applied.

$$\frac{\sigma(T_{1/2})}{T_{1/2}} \approx \frac{2}{\lambda T}\cdot\sqrt{\frac{3\cdot(n-1)}{n\cdot(n+1)}}\cdot\frac{\sigma(A)}{A} \qquad [5]$$

In the case of high-frequency components, n is the number of measurements. In the case of medium-frequency deviations, it is the number of periods covered by T, the duration of the measurement campaign. $\sigma(A) = \sqrt{N}$ is the uncertainty of the decay rate for the two gamma spectrometry systems and $\sigma(A) = \sigma(I)$ for the ionization chamber is the uncertainty of the measured current. For the rest of components the relative uncertainty of the component under study was used. Finally, for low-frequency instabilities the propagation factor is $2/\lambda T$.

- *High-frequency deviations*

The high-frequency perturbations are identified as those occurring at a rate comparable to the number of measurements per campaign. For the CIR measurement this component is the standard deviation of the residuals while for the $CeBr_3$ measurements it is the counting statistics. In all cases, the propagation factor was calculated as:

$$F = \frac{2}{\lambda T}\cdot\sqrt{\frac{3\cdot(n-1)}{n\cdot(n+1)}} \qquad [6]$$

with n representing the number of measurements performed in each case.

- *Medium-frequency deviations*

Once the deviation due to dead-time in the case of $CeBr_3$ analogue counting was corrected for, the only medium-frequency perturbation observed was the sinusoidal oscillation in the residuals, which was accounted for with the propagation factor calculated as formula [4], with n expressed as the number of periods of the oscillation covered by the measurement campaign.

- *Low-frequency deviations*

These sources of uncertainty were background and timing for all three methods and the standard deviation of the mean value calculated for the $CeBr_3$ digital method from applying different dead-times.

The first two components were estimated using the Monte Carlo method explained in (JGCM, 2008). 10^4 fits were performed using the Levenberg–Marquardt algorithm and for each fit, the parameter in question (background/timing) was varied stochastically within its

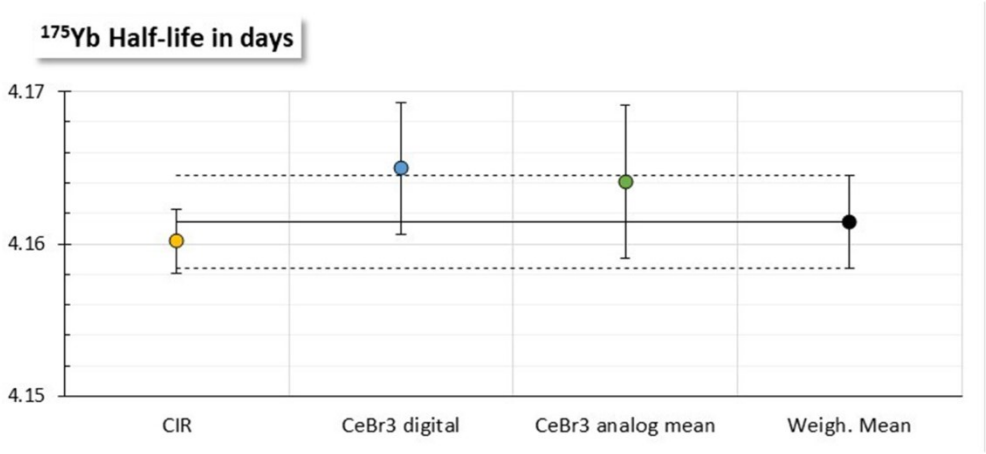

Fig. 10. ^{175}Yb half-life values with uncertainties ($k = 1$) obtained with each measurement method and weighted mean of all three values.

uncertainty distribution, assumed as Gaussian. The average of the half-life distribution thus obtained, was assumed to be the actual half-life and the standard deviation of this distribution was estimated to be the half-life uncertainty stemming from the component under study.

4.2. ^{175}Yb half-life

The weighted mean of the values from each technique was calculated to obtain the ^{175}Yb half-life, thus the differences between the measurement techniques and their characteristics were taken into account proportionately. Fig. 10 presents the individual values and the weighted mean showing their compatibility. The corresponding uncertainty was estimated by performing an additional budget where the median of high and low-frequency components together with the standard deviation of the weighted mean were taken into account. The final value and associated uncertainty for ^{175}Yb half-life is 4.1615(30) days.

The only two documented references of ^{175}Yb half-life state 4.185(1) days (ENSDF 2004; Abzouzi et al., 1989) and 4.19(1) days (Wien, 1966) with no detailed information about the measurement procedures or uncertainty evaluations. The value presented in this work deviates by 0.56% from the precedent nuclear reference value (ENSDF 2004) and is supported with an exhaustive calculation of the associated uncertainty.

5. Conclusions

A new measurement of the ^{175}Yb half-life was carried out using three independent measurement systems. These measurements were validated by the measurements of the half-lives pf ^{177}Lu and ^{99m}Tc. A thorough uncertainty assessment was performed taking the different frequency range deviations relative to the length of the measurement campaign into account. The half-life of ^{175}Yb was determined as the weighted mean value of the results obtained from the three methods using the decay curve fitting procedure. The result obtained is $T_{1/2}(^{175}\text{Yb}) = 4.1615(30)$ days, corresponding to a relative standard uncertainty of 0.07%.

Funding

Zeynep Talip and Nick van der Meulen received funding from the Swiss National Science Foundation (SNF Grant Number: 200021_188495).

Declaration of competing interest

The authors declare that they have no known competing financial interests or personal relationships that could have appeared to influence the work reported in this paper.

References

Abzouzi, A., Antony, M.S., Ndocko Ndongué, V.B., 1989. Precision measurements of the half-life of nuclides. Journal of Radioanalytical Nuclear Chemistry, Letters 135 (1), 1–7.

Advanced Accelerator Applications (AAA). https://www.adacap.com.

Aghaei-Amirkhizi, N., Moghaddam-Banaem, L., Athari-Allaf, M., Sadjadi, S., Johari-Daha, F., 2016. Development of dendrimer encapsulated radio-ytterbium and biodistribution in tumor bearing mice. IEEE Transactions on Nanobioscinence 15 (6), 549–554.

Aghanejad, A., Jalilian, A.R., Bahrami-Samani, A., Shirvani-Arani, S., Moradkhani, S., 2014. Radiosynthesis and evaluation of ytterbium-175 labeled bleomycin as therapeutic agent. Iran. J. Nucl. Med. 22 (2), 40–45.

Browne, E., Tuli, J.K., 2017. Nuclear data Sheets for A = 99. Nucl. Data Sheets 145, 25–340.

Chakraborty, S., Unni, P.R., Venkatesh, M., Pillai, M.R.A., 2002. Feasibility study for production of Yb-175: a promising therapeutic radionuclide. Appl. Radiat. Isot. 57 (3), 295–301.

DCF77, 2021. https://www.schwille.de/wp-content/uploads/860-000-beschreibung.pdf.

Duchemin, C., et al., 2020. CERN-MEDICIS : a unique facility for the production of non-conventional radionuclides for the medical research. In: 11th International Particle Accelerator Conference (IPAC2020). JACoW Publishing, Caen, France.

Duran, M.T., et al., 2020. Determination of ^{161}Tb half-life by three measurement methods. Appl. Radiat. Isot. 159, 109085.

Gostely, J.-J., Carnal, E., 1978. La méthode des deux oscillateurs pour la mesure du temps mort dans l'instrumentation nucléaire. Nucl. Instrum. Methods 150 (3), 459–464.

Jamre, M., Shamsaei, M., Maragheh, M.G., Sadjadi, S., 2019. Novel Yb-175-Poly (L-Lactic acid) microspheres for transarterial radioembolization of unrespectable hepatocellular carcinoma. Iran. J. Pharm. Res. (IJPR) 18 (2), 569–578.

JGCM, 2008. Evaluation of Measurement Data - Supplement 1 to the "Guide to the Expression of Uncertainty in Measurement" - Propagation of Distributions Using a Monte Carlo Method.

Juget, F., Nedjadi, Y., Buchillier, T., Bochud, F., Bailat, C., 2016. Determination of ^{137}Cs half-life with an ionization chamber. Appl. Radiat. Isot. 118, 215–220.

Kondev, F.G., 2019. Nuclear data Sheets for A = 177. Nucl. Data Sheets 98 (4), 801–1095.

Mathew, B., Chakraborty, S., Das, T., Sarma, H.D., Banerjee, S., Samuel, G., Venkatesh, M., Pillai, M.R.A., 2004. Yb-175 labeled polyaminophosphonates as potential agents for bone pain palliation. Appl. Radiat. Isot. 60 (5), 635–642.

Pommé, S., 2015. The uncertainty of the half-life. Metrologia 52, 51–65.

Pommé, S., Camps, J., Van Ammel, R., Paepen, J., 2008. Protocol for uncertainty assessment of half-lives. J. Radioanal. Nucl. Chem. 276 (2), 335–339.

Shamsuzzoha Basunia, M., 2004. Nuclear data Sheets for A = 175. Nucl. Data Sheets 102, 719–900.

Talip, Z., Borgna, F., Müller, C., Ulrich, J., Duchemin, C., Ramos, J.P., Stora, T., Köster, U., Nedjadi, Y., Gadelshin, V., Fedosseev, V.N., Juget, F., Bailat, C., Fankhauser, A., Wilkins, S.G., Lambert, L., Marsh, B., Fedorov, D., Chevallay, E., Fernier, P., Schibli, R., van der Meulen, N., 2021. Production of mass-separated Erbium-169 towards the first preclinical in vitro investigations. Front. Med. 8. Article Number 643175.

Vaez-Tehrani, M., Zolghadri, S., Afarideh, H., Yousefnia, H., 2016. Preparation and biological evaluation of Yb-175-BPAMD as a potential agent for bone pain palliation therapy. J. Radioanal. Nucl. Chem. 309 (3), 1183–1190.

Vahidfar, N., Jalilian, A.R., Fazaeli, Y., Aghanejad, A., Bahrami-Samani, A., Alirezapour, B., Erfani, M., Beiki, D., Khalaj, A., 2014. Development of

radiolanthanide labeled porphyrin complexes as possible therapeutic agents in beast carcinoma xenografts. Radiochim. Acta 102 (7), 659–668.
Wang, Meng, Huang, W.J., Kondev, F.G., Audi, G., Naimi, S., 2021. The AME202 atomic evaluation. Chin. Phys. C 45 (3), 030003.
Wien, K., 1966. Der Zerfall von ^{174}Tm und ^{175}Tm. Z. Phys. 191, 137–159.